Building and Environment 87 (2015) 117–128

Contents lists available at ScienceDirect

Building and Environment

journal homepage: www.elsevier.com/locate/buildenv

Upper room UVGI effectiveness with dispersed pathogens at different droplet sizes in spaces conditioned by chilled ceiling and mixed displacement ventilation system

Mohamad Kanaan [a], Nesreen Ghaddar [a, *], Kamel Ghali [a], George Araj [b]

[a] Department of Mechanical Engineering, American University of Beirut, PO Box 11-236, Beirut 11072020, Lebanon
[b] Department of Pathology & Laboratory Medicine, American University of Beirut, Beirut, Lebanon

ARTICLE INFO

Article history:
Received 31 October 2014
Received in revised form
12 January 2015
Accepted 28 January 2015
Available online 7 February 2015

Keywords:
Bacteria distribution
Disease transmission
Mathematical modeling
CFD modeling
Air sampling
Settling petri plates

ABSTRACT

This paper investigates by modeling and experimentation the dispersion of bacteria and performance of Upper Room Ultraviolet Germicidal Irradiation (*UVGI*) in spaces conditioned by combined chilled ceiling (*CC*) and mixed displacement ventilation (*DV*) system. The effects of gravitational settling and deposition were taken into account in mathematical modeling to reasonably simulate the transport of pathogen via expiratory droplets of all size ranges. The model was experimentally validated with and without the use of *UVGI* for different ventilation rates. Experiments were conducted in a *CC/DV* test room with a constant generation of *Serratia marcescens*, an extremely UV-susceptible microorganism to measure the airborne bacteria concentration in the room air and quantify the bacteria deposition on horizontal surfaces. The experimental bacteria colony forming units (*CFU*) count was used to validate a *CFD* model developed to predict the deposition of pathogen carriers. The mathematical model was then substantiated using the *CFD* predictions of pathogen concentration in the space for large carrying particles. The validated mathematical model was then used to study the effect of pathogen-carrying particle sizes on the microbiological indoor air quality. Results showed that the droplet size affects the value of maximal bacteria concentration and the height at which it occurs. Moreover, the UV disinfection rate achieved in the upper zone decreases from 88% to 78% when the size of pathogen-carrying particles increases from 2.5 μm to 20 μm meaning that greater percentage of bacteria are removed by deposition when bacteria is carried by large particles.

1. Introduction

The use of return air in air-conditioning systems is intended to save energy by decreasing the cooling load, but will result in an increase in the concentrations of air pollutants including particulates and microbial contaminants. Bioaerosols such as bacteria and viruses are part of indoor particulate matters and might pose an environmental hazard when present in high concentrations in indoor environments causing health issues of occupants [1,2]. Therefore, limitations should be imposed to the return air fraction in order to maintain healthy air quality and prevent cross-infection in indoor environments. WHO (1988) [3] recommended that bacteria concentration in office spaces not to exceed 500 CFU/m^3 bacteria in office spaces, while no more than 200 CFU/m^3 is allowed in hospitals.

The chilled ceiling and displacement ventilation (*CC/DV*) system is one of the ventilation systems that is known for its effectiveness in providing high indoor air quality at a lower energy cost and is widely used in office buildings [4,5]. In this system, the cold air is supplied at relatively low velocity, spreads over the floor, moves upwards, and then is exhausted at the ceiling level. The warm exhaled air which may carry pathogens will then rise upward and will circulate in the upper mixing zone of the room. The use of mixed supply air in the *CC/DV* system has been shown to improve energy performance by 27% when return air mixing ratio is about 30% while keeping the bacteria concentration in the breathing air layer at the standard limit of 500 CFU/m^3 [6].

One of the effective methods used for reducing the airborne bacteria concentration in buildings without bringing in fresh air is the upper room ultraviolet germicidal irradiation (*UVGI*) [7–9]. This

* Corresponding author. Tel.: +961 1350000x2513; fax: +961 1 363283.
E-mail address: farah@aub.edu.lb (N. Ghaddar).

http://dx.doi.org/10.1016/j.buildenv.2015.01.029
0360-1323/

Nomenclature

A	area, m^2
$\bar{c}$	normalized bacteria count, CFU
c_d	drag coefficient
c_s	Cunningham–Stokes slip correction factor
C_b	airborne bacteria concentration, CFU/m^3
CFU	colony forming unit
d	diameter, m
D	molecular diffusivity in air, m^2/s
D_t	turbulent diffusivity in air, m^2/s
D_{UV}	*UV* dose, J/m^2
E	*UV* irradiance, W/m^2
F_L	lift force, N
H_s	stratification height, m
KR	killing rate
m	mass flow rate, kg/s
n	Brownian motion
N	average number of bacteria colonies per liter of solution, CFU/L
q_b	bacteria generation rate, CFU/min
Q	sampling air flow rate, m^3/min
r	radial coordinate, m
S	microorganism survival rate
Sc	Schmidt number
t	exposure time to *UV*, s
T	temperature, °C
T_{ext}	total air sampling time, min
u	velocity, m/s
u^*	friction velocity, m/s
V	volume, m^3
v_d	deposition velocity, m/s
v_s	settling velocity, m/s
W	wall width, m
z	layer elevation from floor level, m
z_m	mid-layer height
z_t	plume terminal height, m
z_{UV}	UV-zone starting height, m
Y	wall thickness, m
Z	*UV* susceptibility, m^2/J

Greek symbols

β	mixing factor
Φ	source heat flux, W
ρ	density, kg/m^3
μ	fluid dynamic viscosity, kg/(m s)
δ	particle-fluid density ratio
ν	air kinematic viscosity, m^2/s
λ	gas molecular mean free path

Subscripts

a	air
c	ceiling
d	deposition
ent	entrained
ex	exchange
f	floor
gen	generation
int	interface
k	layer number
p	plume
s	supply
t	terminal
w	wall

method consists to irradiate the air in the upper room with ultraviolet light while providing mixing between the upper irradiated zone and lower occupied zone. Airborne pathogens are mostly susceptible to ultraviolet radiation of wavelength of 254 nm, which damages the nucleic acids of the microorganism. The use of upper room *UVGI* in *CC/DV* spaces allows significant fractions of return air since the latter will be effectively disinfected due to the air recirculation in the upper *UV* zone before leaving the space and being reused in the *DV* supply.

Human occupancy is a major indoor source of bioaerosols. Expiratory activities of Humans such as breathing, speaking, laughing, coughing, and sneezing, result in the introduction of droplets with infectious content in the indoor air. Each of these processes generates droplets of different sizes and pathogen concentrations. Published experimental cough and sneeze droplet size distribution data showed that the emitted particles may vary in size from 1 μm to greater than 100 μm [10–12]. In more recent studies, interferometric Mie imaging (IMI) technique was used to determine the size distributions of expiratory droplets expelled during coughing and speaking. It was reported that the geometric mean diameter of droplets from coughing was 13.5 μm and it was 16.0 μm for speaking [13]. It is also worth to mention that an emitted particle can rapidly undergo a water loss to an equilibrium diameter that is approximately one-half the initial diameter [14]. The equilibrium size means the diameter of a droplet for which there is no net change in water content. Two modes of disease transmission were then identified: “Airborne” and “Droplet” [15]. In the “Airborne” mode, the pathogen carriers are droplet nuclei of 1–5 μm that remain suspended in the air for prolonged periods of time [16,17]. The term “droplet nucleus” refers to the dried residue of a droplet [18]. However, it was reported that droplets larger than 20 μm cannot become droplet nuclei [14] and may be pathogen-carrying particles in the “Droplet” mode of disease transmission. In this mode, the pathogen carriers are droplets of larger equilibrium sizes (>5 μm) that can be removed from air by gravitational settling and deposition onto solid surfaces, and then transferred by touch to new patients.

Although a few research studies addressed modeling the dispersion of airborne pathogen in indoor environments a large number of models were developed in the literature to predict the performance of upper room *UVGI* in disinfecting indoor air. Modeling approaches to study efficacy of upper-room *UVGI* either used *CFD* or simplified multi-zone-mixing models. Hathway et al. [19] evaluated using *CFD* modeling the risk from the transport of infectious bioaerosols in spaces with conventional air conditioning. Heidarinijad and Srebric [20] presented different *CFD* modeling methods of upper room *UVGI* effectiveness. The obtained *CFD* results were then compared with existing experimental studies. Noakes et al. [7] developed analytical two-zone and three-zone mixed models with the air in each zone being fully mixed, but with incomplete mixing between the zones. The mixing coefficients between zones were determined using the inter-zonal velocities found either by measurements or *CFD*. The model results were compared with *CFD* values and good agreement was reported for suitable mixing factors. Habchi et al. [21] developed a simplified model to predict the active particle behavior in *DV* spaces. They concluded that the ventilation flow rate should be sufficiently high to overcome the gravitational settling of particles and then prevent the stratification in particle concentration from occurring at the breathing level. Kanaan et al. [6] developed an airborne bacteria transport plume-multi-layer zonal model to predict bacteria distribution in combined chilled ceiling (*CC*) mixed displacement ventilation (*DV*) without and with upper-room *UVGI* installed. The comparison of the model results with the predictions of experimentally-validated computational fluid dynamics (*CFD*) simulations revealed good agreement with maximal error of ± 10.4 CFU/m^3. However, this model applicability is limited to the "Airborne" mode where the pathogen-carrying particles are droplet nuclei that are affected purely from the ventilation air flow, and as a result, gravitational settling and deposition were neglected. But, as the diameter of a particle increases, the gravitational settling effect increases acting against the upward air motion and thus challenging the performance of the *DV* system. The gravitational effect will also minimize the pathogen exposure to *UV* irradiation in the upper room resulting in low effectiveness of upper room *UVGI*. It is not also clear how the increase in deposition of pathogens droplets would affect the maximum return air ratio of the mixed displacement ventilation since bacteria elimination in room air has two paths, one by *UV* irradiation and the other by deposition on surfaces.

The aim of this work is to build a robust mathematical model for *CC/DV* spaces with upper room *UVGI* that can be used to assess not only "airborne" disease transmission, but also the "droplet" mode in which pathogens are carried by large expiratory droplets that may deposit on surfaces and cause infections by direct physical contact. The gravitational settling and deposition of droplets are taken into account to improve the accuracy of predictions of the multilayer multi-zone model for airborne pathogen transport in *CC/DV* spaces with upper room *UVGI*. The most important distinction from the earlier model [6] is the inclusion of bacteria deposition on surfaces as this represents an important mechanism for decreasing bacterial cross-contamination through: i) a direct path by decreasing the bacteria concentration in breathable air and an indirect path by depositing bacteria at surfaces away from the healthy occupant. The current model will be validated by experimentation for bacteria of small sizes and then substantiated using *CFD* Lagrangian tracking for large size bacteria. The validated model is then used to determine the effect of droplet size on pathogen distribution and performance of upper room *UVGI* in *CC/DV* spaces.

2. Methodology

In order to assess airborne disease transmission in mixed *CC/DV*-conditioned spaces, we consider 1-D plume-multi-layer mathematical modeling of the transport and deposition of airborne pathogens at different sizes of carrying particles. An experimental validation of 1-D model follows where the concentration of airborne pathogen in the indoor air is measured and then compared with numerical predictions for small airborne droplet nuclei size without and with the use of the *UVGI*. Furthermore, a three-dimensional *CFD* model is developed and validated by the same experimental set up for accurate prediction of deposition and concentration in the simulated space. The validated *CFD* model is then used to validate the 1-D mathematical model predictions for the behavior of large droplets and to use the 1-D model to study the effect of different size particles on the effectiveness of the *UVGI* system in mixed *CC/DV* conditioned spaces and the impact on the maximum allowable mixing ratio that meet air quality constraints.

2.1. Mathematical modeling

In displacement ventilated spaces, the velocity field is set up with the vertical plumes generated by the heat sources. Air pollutants such as particulate matters and gases are transported by this velocity field and by diffusion. Saliva droplets that are larger than 20 μm rapidly settle onto surfaces [22], while droplets between 0.5 and 20 μm remain in the air for long periods and are more likely to be captured in the respiratory tract and produce infection [23]. The driving force of the plume is the temperature difference between the plume and the surroundings. When this difference diminishes, the plume reaches its terminal height at which it spreads horizontally to delimit an upper mixing zone. Two zones with opposite unidirectional flows are identified below the plume terminal height in the surroundings of the plume. The interface between the two zones is called the stratification height and is defined as the level where the air flow rates of plume and wall plumes are balanced with the supply air flow rate. The current multilayer model is coupled with the thermal space multilayer model for CC/DV spaces [24] where the radiation heat transfer exchange was considered between the ceiling and walls and between the occupants and the space surfaces (walls and chilled ceiling) for thermal comfort evaluation.

The *UVGI* space conditioned by *CC/DV* system is conceptually divided into the following seven air zones as shown in Fig. 1 and as introduced in Ref. [6]: floor zone, stratification zone, wall plume zone, thermal plume zone, two room air zone outside plumes (below and above the stratification level), lower mixed-air zone, and upper mixed air *UV* zone. The exhaust flow rate is taken to be always higher than the supply rate by 5% to maintain a negative pressure in the *CC/DV* space.

A cylindrical heat source is replaced by a virtual point as explained in Ref. [25]. The mass flow rates of the plumes from heat sources ($\dot{m}_p$) are computed using the following correlations [26] where Φ is the source heat power and dT/dz is the vertical temperature gradient of room air.

$$\dot{m}_p = 0.00238\Phi^{3/4}(dT/dz)^{-5/8}B_1 \tag{1a}$$

$$\begin{aligned} B_1 &= 0.004 + 0.039A_1 + 0.38A_1^2 - 0.062A_1^3 \quad \textit{and} \\ A_1 &= 2.86z(dT/dz)^{3/8}\Phi^{-1/4} \end{aligned} \tag{1b}$$

The mass flow rates of wall plumes ($\dot{m}_w$) are given by Jaluria [27] as:

$$\dot{m}_w = 2.87 \times 10^{-3}\rho(\Delta T_w)^{1/4}z^{3/4}Y \tag{2}$$

where Y is the wall width and $\Delta\theta_w$ is the wall-air temperature difference. The plume terminal height (z_t) is given in Ref. [26] as follows:

$$z_t = 0.74\Phi^{1/4}(dT/dz)^{-3/8} \tag{3}$$

The net circulated flow rate ($\dot{m}_{cir}$) at each height z representing the layer height is calculated as

$$\dot{m}_{cir} = \dot{m}_s - \sum_{i=1}^{n}\dot{m}_{p,i} - \sum_{j=1}^{h}\dot{m}_{w,j} \tag{4}$$

where n is the number of heat sources and h is the number of room walls. Wall temperatures are assumed to be always higher than the room air temperature.

In order to provide accurate predictions of airborne pathogen concentration, the model should account for the principal physics that affect the particle/bacteria behavior such as convection, molecular and turbulent diffusion, deposition, and gravitational settling. For pathogen-carrying droplets smaller than 20 μm, the deposition effect may be neglected as droplets in this size range evaporate quickly and remain in the air for long periods of time. However, the inclusion of gravitational settling and deposition is

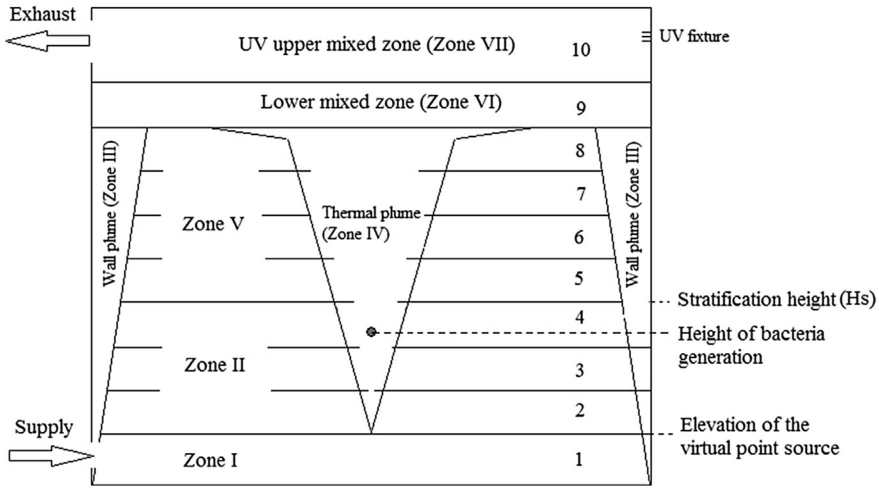

Fig. 1. Schematic of model air zones and layers [6].

necessary when modeling larger particles that may settle rapidly onto surfaces. It was assumed that all the surfaces in the modeled space are either horizontal or vertical. The deposition velocities including the Brownian and turbulent diffusion in addition to the gravitational settling effect on particle behavior for vertical walls, floor, and ceiling are given respectively by the following expressions [28]:

$$v_{d,w} = \frac{u^*}{I} \tag{5a}$$

$$v_{d,f} = \frac{v_s}{1 - \exp\left(\frac{-v_s I}{u^*}\right)} \tag{5b}$$

$$v_{d,c} = \frac{v_s}{\exp\left(\frac{v_s I}{u^*}\right) - 1} \tag{5c}$$

where v_s is the settling velocity calculated using the saliva droplet density and equilibrium size, and air dynamic viscosity as follows:

$$v_s = \frac{\rho d_p^2 g}{18\mu} \tag{5d}$$

I is an integral number given by:

$$I = 3.64 Sc^{2/3}(a - b) + 39 \tag{5e}$$

$$a = \frac{1}{2}\ln\left[\frac{\left(10.92Sc^{-1/3} + 4.3\right)^3}{Sc^{-1} + 0.0609}\right] + \sqrt{3}\arctan\left[\frac{8.6 - 10.92Sc^{-1/3}}{10.92\sqrt{3}Sc^{-1/3}}\right] \tag{5f}$$

$$b = \frac{1}{2}\ln\left[\frac{\left(10.92Sc^{-1/3} + r^{+3}\right)}{Sc^{-1} + 7.669e^{-4}\left(r^+\right)^3}\right] + \sqrt{3}\arctan\left[\frac{2r^+ - 10.92Sc^{-1/3}}{10.92\sqrt{3}Sc^{-1/3}}\right] \tag{5g}$$

u* is the friction velocity with a typical value of 1.5 cm/s in indoor environments.

After including gravitational settling and deposition of the pathogen-carrying particles, the steady-state airborne bacteria mass balance for Layer 1 adjacent to the floor is given by:

$$\dot{m}_s C_{b,s} + A_1 \rho v_s C_{b,2} + A_1 \rho D \left(\frac{\partial C_b}{\partial z}\right)_1 = \left(\dot{m}_s + \rho v_{d,f} A_f + \sum_{j=1}^{h} \rho v_{d,w,1} A_{w,j,1}\right) C_{b,1} \tag{6}$$

In the above equation, $C_{b,s}$ is the airborne bacterial concentration in the supply air stream. The second term on the left side of Eq. (6) is diffusion through the interface of area A_1 with Layer 2, D is the molecular diffusion coefficient, and v_s is the droplet settling velocity. A_f and $A_{w,j,1}$ are respectively the floor area and surface area of the wall j within Layer 1. $v_{d,f}$ and $v_{d,w,1}$ are the particle deposition velocities on the floor and the walls within Layer 1 respectively.

The bacteria mass balance for the air layer k ($k = 2$–8) is given by:

$$\left(\dot{m}_{cir,k-1} + \sum_{j=1}^{h} \dot{m}_{w,j,k-1}\right) C_{b,k-1} - A_{\text{int},k}(D + D_t)\rho\left(\frac{\partial C_{b,p}}{\partial r}\right)_{zm_k} + A_k \rho v_s C_{b,k+1} + A_k \rho D \left(\frac{\partial C_b}{\partial z}\right)_{zm_k, zm_{k+1}} = \left(\dot{m}_{cir,k} + \dot{m}_{ent,k} + A_{k-1}\rho v_s + \sum_{j=1}^{h} \dot{m}_{w,j,k} + \sum_{j=1}^{h} \rho v_{d,w,k} A_{w,j,k}\right) C_{b,k} + A_{k-1}\rho D \left(\frac{\partial C_b}{\partial z}\right)_{zm_{k-1}, zm_k} \tag{7}$$

The first term in the left side of Eq. (7) is the convective term associated with air transport and the second term is the diffusion between the plume and adjacent air layer at the middle of that layer. The bacterial concentration inside the plume is $C_{b,p}$, r is the radial coordinate from the plume centerline, $\dot{m}_{ent}$ is the mass entrained by the plume from the adjacent air layer, and D_t *is* turbulent diffusion coefficient that was correlated to plume upward velocity and characteristic turbulent length that is the plume width at any height [29].

The bacteria mass balance inside the plume in layer k ($k = 2–8$) is given by:

$$\begin{aligned}&\dot{m}_{p,k-1}C_{b,p,k-1}+\dot{m}_{ent,k}C_{b,k}+\rho q_{b,k}+A_{p,k}\rho v_s C_{b,p,k+1}\\&+A_{p,k-1}D\rho\left(\frac{\partial C_{b,p}}{\partial z}\right)_{zm_{k-1},zm_k}=A_{p,k-1}\rho v_s C_{b,p,k}\\&-A_{\text{int},k}(D+D_t)\rho\left(\frac{\partial C_{b,p}}{\partial r}\right)_{zm_k}+A_{p,k}D\rho\left(\frac{\partial C_{b,p}}{\partial z}\right)_{zm_k,zm_{k+1}}\\&+\dot{m}_{p,k}C_{b,p,k}\end{aligned} \tag{8}$$

where $\dot{m}_p$ is the mass flow rate of the plume at the boundary, A_p is the plume area at the interface, and $q_{b,k}$ is the volumetric bacteria flow rate generated in layer k where $q_{b,k}$ is q_b for $k = 4$ and zero otherwise.

The bacteria mass balance in Layer 9 which is the lower mixing zone of the fully-mixed region described previously is given by the following equation where β is the mixing factor defined in Ref. [13].

$$\begin{aligned}&\left(\sum_{j=1}^{h}\dot{m}_{w,j,8}\right)C_{b,8}+\beta\dot{m}_s C_{b,10}+A_9\rho v_s C_{b,10}+A_{p,8}D\rho\left(\frac{\partial C_{b,p}}{\partial z}\right)_{zm_8,zm_9}\\&=\left[(1+\beta)\dot{m}_s+\dot{m}_{cir,9}+A_8\rho v_s+\sum_{j=1}^{h}\rho v_{d,w,9}A_{w,j,9}\right]C_{b,9}\\&\quad+A_8 D\rho\left(\frac{\partial C_b}{\partial z}\right)_{zm_8,zm_9}\end{aligned} \tag{9}$$

In order to model the inactivation of airborne bacteria using upper room *UVGI*, the average *UV* irradiance in the upper zone is evaluated using the mathematical predictive model of Wu et al. [30] for louvered *UV* lamps. This model is based on thermal radiation view factors, which define the amount of diffuse radiation transmitted from one surface to another. The irradiation reflected by the room surfaces was neglected assuming diffusive enclosures. Although this *UV* model was used and experimentally validated by the authors in previous *UVGI* research study [6], the *UV* irradiance field in the simulated space will be also measured.

The bacteria mass balance in the *UV* upper zone (Layer 10) is then given by

$$(1+\beta)\dot{m}_s C_{b,9}=\left(\beta\dot{m}_s+\dot{m}_e+A_9\rho v_s+A_c\rho v_{d,c}+\sum_{j=1}^{h}\rho v_{d,10}A_{w,j,10}+\rho ZEV_u\right)C_{b,10} \tag{10}$$

where A_c is the ceiling area and $v_{d,c}$ is the bacteria deposition velocity on the ceiling. The term ZEV_u is the *UV* bacteria inactivation term where Z is the bacteria susceptibility to *UV* assumed constant for small variations of relative humidity, E is the average *UV* irradiance in the upper zone, and V_u is the volume of that zone.

2.2. Experimental methodology

The objective of the experiments is to measure the airborne bacteria concentration in an experimental *CC/DV* to validate the mathematical model of pathogen transport and inactivation with *UVGI*. The experimentation also aims to measure the bacteria deposition in the *CC/DV* space with and without the use of *UVGI*.

2.2.1. Experimental facility

Experiments were conducted in a fully-controlled *CC/DV* test room available at the laboratories of the American University of Beirut (AUB) with dimensions 2.75 m (L) × 2.5 m (W) × 2.8 m (H) and two 18 W UVC lamps (Fig. 2). The test room was equipped with a mechanical ventilation system that can deliver up to 0.2 m^3/s of high efficiency particulate air (HEPA) filtered outdoor air through a rectangular grill near the floor level. A negative pressure of about 20 Pa was maintained inside the room. Infiltrated air into the experimental room would carry negligible amount of bacteria since this type of bacteria does not usually exist in the outside environment and its amount would be extremely small compared to the experimentally generated bacteria amounts inside the climatic room. Two 3-way control valves are implemented in the supply line to control panel temperature and inlet water temperature to the fan coil unit that cools supply air from outdoor environment to the desired supply value. The chilled ceiling is composed of three copper tube and plate panels that cover the whole room ceiling area and its temperature is controlled using an electric heater. Occupants are simulated by heated cylinders of diameter 0.3 m and height 1.2 m each having a heat load of 100 W.

An anemometer system (Model IFA 300 16 channels, accuracy 0.15%) equipped with a xyz traverse table was used to mount the probes in order to measure air velocity at different points in the room. Air temperature was also measured at several positions in the room using a type T thermocouple linked to the anemometer system [6].

Two louvered 18 W UVC lamps (A and B) of length 35.6 cm and diameter 1.54 cm (*Dinies*, Germany) were installed at a height of 2.5 m on two opposite walls. Actinometrical cells were uniformly distributed at 1 m from the floor to measure the *UV* irradiance in at the eye level, and at heights 2.2 m and 2.4 m to measure the *UV* field in the upper irradiated zone. The actinometrical cells are filled with a solution prepared by adding 1 g of potassium iodide to 10 ml of the prepared solution of 0.6 M iodide and 0.1 M iodate in 0.01 M borate [31]. This solution is optically opaque at 254 nm and insensitive to room light.

Four experiments were performed at steady-state conditions at two different *DV* supply flow rates with and without the use of *UVGI*. The desired set point temperature was 24 °C and the relative humidity was controlled to be in the thermal comfort zone (40–60%) and constrained further to prevent condensation on the chilled ceiling. Therefore, the effect of RH on bacteria *UV* susceptibility was neglected and a constant value of Z = 0.57 m^2/J was used for *Serratia marcescens* at RH between 40 and 60% [32]. The supply conditions for the experiments were determined using the *CC/DV* design charts [33] for thermal comfort and indoor air quality. The charts are based on the ratio of the *CC* cooling load to the total sensible load, the thermal comfort represented by the temperature gradient, and the amount of displaced air parameter. The supply conditions along with the room temperatures are summarized in Table 1. The used CC temperatures were towards the lower end values normally implemented in practice to prevent condensation on the chilled ceiling where CC temperature is always kept higher than the dew point temperature of adjacent indoor air.

Before starting each experiment, the room should be flushed using HEPA-filtered ventilation air for 3 h without recirculating any

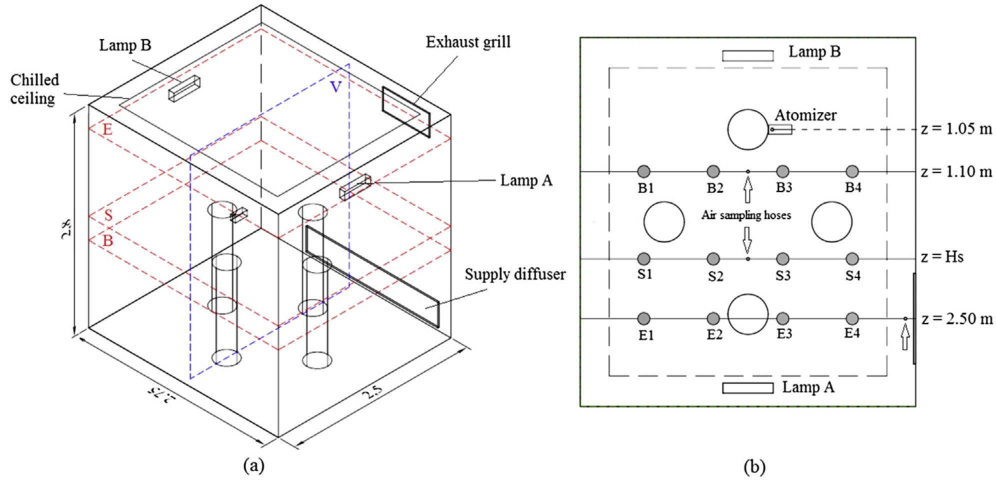

Fig. 2. Schematics of the *CC/DV* room (a) isometric view showing the vertical sampling plane (V) and horizontal planes (B, S, and E), and (b) top view showing the locations of the air sampling hoses. *Hs* denotes the stratification height.

return air. Some experiments were repeated twice to ensure repeatability of the measurements. The error in concentration measurements and *CFU* counts for any repeated experiment was less than 9%.

2.2.2. Measurements of airborne bacteria concentration and bacteria settling

The performance of the *UVGI* system was tested using the constant bacteria generation method. A suspension of *S. marcescens* (10^8 CFU/mL) freshly prepared in the Department of Pathology at the American University of Beirut Medical Center (AUBMC) was introduced using a six-jet atomizer (Model 9306A, TSI, Inc., USA). The atomizer was located inside the room to avoid the use of long supply hoses where significant deposition of suspension droplets might occur (Fig. 2). The atomized bacteria suspension was released near the top of a heated cylinder 1.05 m above the floor at flow rate 12 L/min and pressure 138 KPa at droplet sizes smaller than 10 μm. The velocity at the atomizer outlet was 0.52 m/s. The damaging effect of aerosolization on the bacteria was neglected. Moreover, *S. marcescens* natural die-off was neglected as it survives for prolonged periods of time under room conditions and as the constant generation method for assessing *UVGI* is used [32,34]. The removal of the bacteria in the current work is then assumed to occur mainly by gravitational settling and *UV* irradiation. In addition, the used size of a pathogen-carrying particle is always taken as the equilibrium diameter of the expiratory droplet. The equilibrium size means the diameter of a droplet for which there is no net change in water content. Please note that the majority of droplets are small in size (more than 80% were <50 μm) and evaporate within seconds under normal room conditions [35].

In order to maintain a constant atomization rate without the need for replenishment during the experiment, the atomizer was filled with a relatively large amount of 350 mL of bacteria suspension. A set of measurements of suspension discharge from the atomizer throughout the experiment duration indicated this amount of bacteria was sufficient. The volumetric flow rate of the suspension leaving the atomizer was about 0.25 mL/min.

The indoor *S. marcescens* concentration was measured using the air sampling method. This method consists to extract a significant volume of air into a sterile solution that will be analyzed to determine the viable bacteria count per unit of air volume. Sampler inlets were placed at three different heights inside the room labeled as follows: the breathing level of a seated adult 1.1 m from the floor (label: B), stratification height (label: S), and room exhaust (label: E).

In each experiment, the bacteria generation was started and maintained for 120 min, and during the last 30 min of generation air samples were collected. The total time taken by an experiment is then 5 h including the room flushing duration.

Air samples were collected using constant flow air sampling pumps (SENSIDYNE, Gilian 5000, USA) at 2.75 ± 0.1 L/min through glass impingers (ACE GLASS, 25 mL) each containing 10 mL of phosphate-buffered saline (PBS) that was autoclaved under a temperature 115 °C for 15 min (Fig. 3). Then, the samples were stored at a low temperature of 4 °C to prevent any bacteria growth prior to incubation.

The impinged liquids were placed onto agar plates that had been incubated at 35 °C for 36 h. The concentration of culturable airborne bacteria (CFU/L) was calculated as:

$$C = \frac{NV}{QT_{ext}} \tag{11}$$

where N is the average number of CFU per liter of the sterile solution (CFU/L), V is the final impinger volume (L), Q is the sampling air flow rate (L/min), and T_{ext} is the total sampling time (min).

In order to measure the bacteria deposition, settle petri plates of standard diameter of 90 mm with a convenient agar-based growth medium were used in the experimental facility. Four plates were evenly distributed and exposed at each of the three aforementioned heights (breathing level, stratification level, and exhaust level) and labeled accordingly as shown in Fig. 2(b). The plates are used to obtain directly the vertical distribution of bacteria deposition and it will help assess the risk of indirect infection by hand-surface contact, especially for surface close to the occupant and the stratification height where accumulation of particles might occur.

The plates were initially covered at the beginning of each experiment, and then uncovered after two hours and kept exposed

Table 1
Experimental scenarios.

Experiment number	Supply air flow rate (kg/s)	Supply air temperature (°C)	Chilled ceiling temperature (°C)	Exhaust air temperature (°C)	Operating UV lamps
I	0.11	20.2	18.3	23.5	None
II	0.11	20.4	18.1	23.4	A and B
III	0.22	21.4	19.5	23.6	None
IV	0.22	21.5	19.6	23.6	A and B

(a) (b)

Fig. 3. Pictures showing the (a) heated cylinders, air sampling hoses, atomizer, and (b) air sampling hoses connected to impingers.

for another two-hour period of time. After incubation, the count of *S. marcescens* colony forming units on each plate was reported to indicate the number of viable bacteria that deposited on each plate. The counting of CFU assumes that every colony is separate and founded by a single viable microbial cell [36].

The disinfection rate achieved by the *UVGI* system is determined as being equal to $1 - S$ where S is the microorganism survival rate defined as:

$$S = \frac{C_{UV,ON}}{C_{UV,OFF}} \tag{12}$$

2.3. CFD modeling

A steady state *CFD* model was developed using ANSYS FLUENT 14.5 to predict the deposition of pathogen-carrying particles in the *CC/DV* test room. The environmental set up including supply, exhaust, microorganism source, and the *UVGI* lamp sizes and positions was kept as close as possible to the real environment. However, there are discrepancies between the experimental set up and *CFD* simulations due to pieces of missing information. The Reynolds averaged Navier–Stokes equations along with standard k-ε were used to simulate turbulent indoor air flow. The surface-to-surface radiation model in ANSYS FLUENT was used to account for radiation exchange between all radiating surfaces.

The domain of the modeled space was discretized into approximately 1,700,000 tetrahedral cells ensuring grid independence and refined at the supply diffuser (Fig. 4). The option of “standard wall function” was activated requiring the y^+ to be within 30 and 300 in the first cell to ensure adequate meshing of the wall turbulent boundary layer containing the particle deposition boundary layer [37]. Mesh quality was ensured with maximum cell skewness less than 0.9. Pressure outlet boundary condition was imposed at the exhaust with a target flow equal to 1.05 times the supply flow rate used in the simulation.

The petri plates were simulated as circular surfaces at the sampling locations and defined as walls in the computational domain. All variables, except the pressure, were discretized with the second-order upwind scheme. STANDARD scheme was used for the pressure term and the SIMPLE scheme was used for coupling pressure and velocity. Numerical convergence was obtained based on many criteria: scaled residuals less than 10^{-5}, stabilized species concentration at the room exhaust, and net imbalance of mass flow less than 1%.

2.3.1. Bacteria transport simulation

Lagrangian Particle tracking with stochastic discrete random walk (*DRW*) model is used to represent the Eddy interactions of the discrete phase. Throughout the literature review, this model can well predict the transport and dispersion of particles and bio-aerosols in indoor environments [19,20]. Pathogen-carrying droplets are simulated as inert spherical particles, 2.5 μm in diameter, with density of 1000 kg/m^3. In this method a large enough number of 100,000 particles were tracked in the simulations to ensure accurate predictions of the stochastic discrete random walk model. Researchers have used spherical shape of droplets for sizes of 20 μm and reported good agreement between experiments and CFD models when considering spherical droplets in the Lagrangian simulations [19]. The shape of the bacteria affects the computed drag but for such a small size particle, drag is very small compared to forced convection upward transport and gravitational forces and the effect of change of drag due to bacteria shape is negligible. Particle trajectories are calculated by a fifth order Runge-Kutta method by considering the change in particle velocity u_{pr} due to drag force, inertia$(u - u_{pr})$, lift force F_L and Brownian motion $n(t)$ thus:

$$\frac{du_{pr}}{dt} = \frac{1}{\tau}\frac{c_d \mathrm{Re}_{pr}}{24}\left(u - u_{pr}\right) + g + F_L + n(t) \tag{13}$$

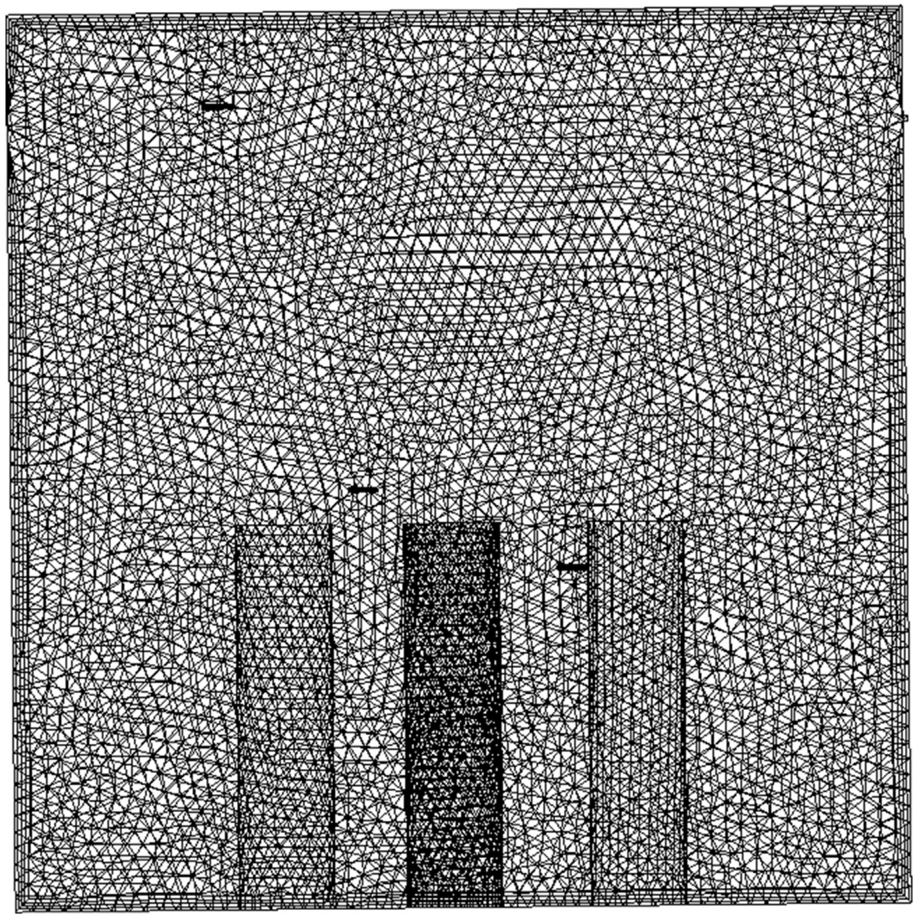

Fig. 4. *CFD* simulation grid at a cut plane.

where τ is the particle relaxation time given by:

$$\tau = \frac{\delta d^2 c_s}{18\nu} \tag{14}$$

where δ is the particle-fluid density ratio, d the particle diameter, ν the fluid kinematic viscosity and c_s is the Cunningham–Stokes slip correction factor given by:

$$c_s = 1 + \frac{2\lambda}{d}\left(1.257 + 0.4\exp\left(-\frac{1.1d}{2\lambda}\right)\right) \tag{15}$$

where λ is the gas molecular mean free path.

The deposition of bacteria was simulated using “trap” boundary condition on the walls and other surfaces in the domain.

2.3.2. *UV irradiance modeling*

The three dimensional predictive *UV* model of Wu et al. [30] was used to integrate the *UV* irradiance field into *CFD* simulations. Local *UV* intensities were implemented into *CFD* control volumes during the post-processing stage. Then, based on the residence time of each particle provided by Lagrangian tracking and the *UV* susceptibility of the microorganism, the received *UV* dose received by each particle was computed as being the *UV* irradiance multiplied by the residence time. A pathogen-carrying particle is deleted when the integrated *UV* dose it has received can achieve bacterial disinfection rate of 90%. This local *UV* irradiance intensity model for bacteria inactivation is performed by developing a supplementary C++ program (user-defined function) that is compiled by the *CFD* software.

3. Results and discussion

This section presents computational and experimental results comparison of *S. marcescens* distributions in the *CC/DV* room described above. The mathematical model predictions of bacteria concentrations are compared with experimental results for the average equilibrium diameter of droplet nuclei (2.5 μm) since the droplets generated by the atomizer have an initial size less than 10 μm meaning that they all become droplet nuclei [14]. Moreover, the *CFD* predictions of deposition of bacteria carriers of the same size are compared to the *CFU* count on the petri plates obtained experimentally. The room was simulated with and without upper room *UVGI* using both *CFD* and mathematical model for all the experimental scenarios.

3.1. *Experimental validation of the mathematical simplified model (for small droplets)*

The values of airborne *S. marcescens* concentrations experimentally found using Eq. (11) compared well with those obtained from the mathematical model with a root-mean-square error (RMSE) of 32.2 CFU/m^3 (Fig. 5); where RMSE had a value of 28.4 CFU/m^3 when the deposition was not included in the modeling. For each set of experiments with the same supply flow

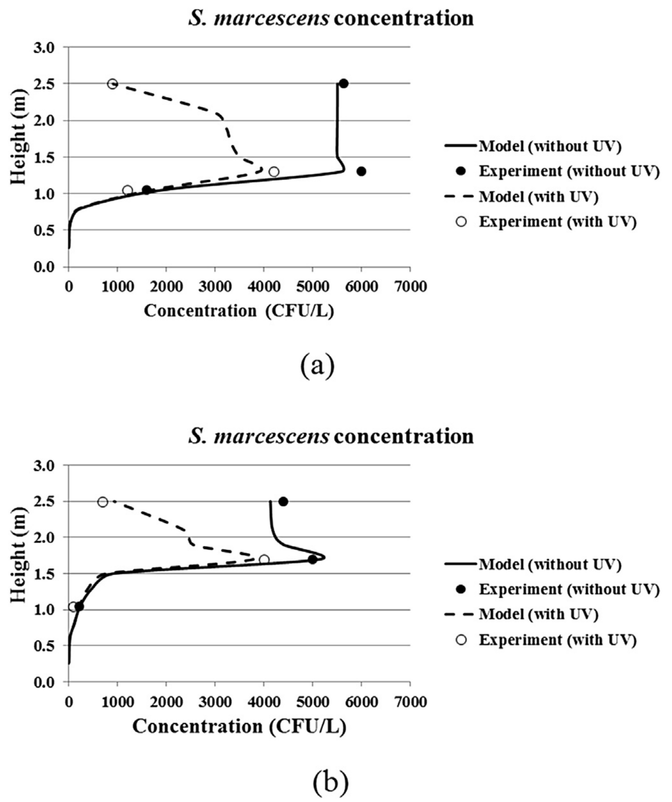

Fig. 5. Comparative plot of measurements and model predictions for *S. marcescens* concentrations for (a) $m_s = 0.11$ kg/s and (b) $m_s = 0.22$ kg/s.

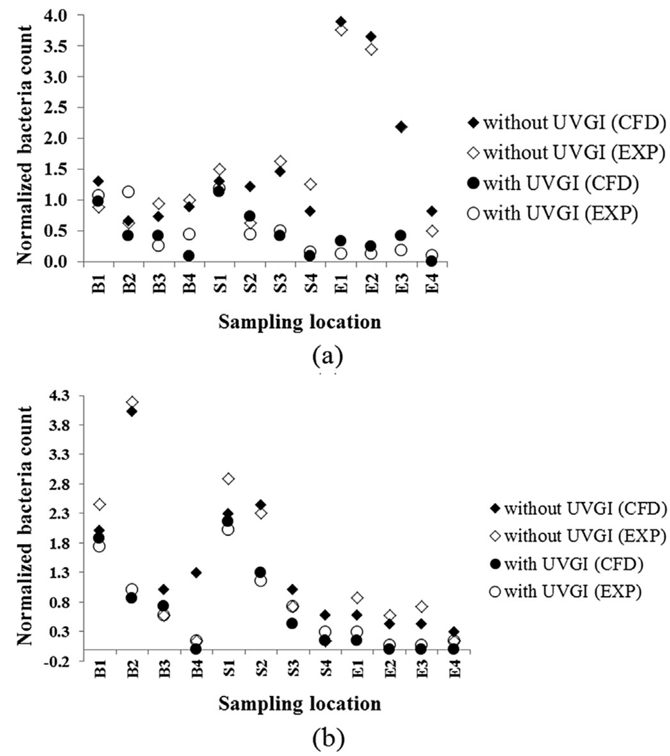

Fig. 6. Comparison between experimental data and numerical bacteria deposition with and without the use of UVGI for (a) $m_s = 0.11$ kg/s and (b) $m_s = 0.22$ kg/s.

rate (I and II, III and IV), the variation of supply temperature did not affect the average temperature in the occupied zone (almost 24 °C). In addition, the supply air is at floor level away from the source generating the bacteria at height of 1.05 m. In addition, the measured exhaust air temperature was almost the same for each set of experiments as shown in Table 1. More improvement on the model prediction accuracy is expected for larger particles where the effects of gravitational settling and deposition might be significant. Although the simulation was run for small droplets where the deposition effect is minimal, the model was able to give reasonable predictions of airborne bacteria concentration at different heights in the room. It can then be confirmed that the particle deposition was well estimated. The plots also show that for higher supply air flow rate the stratification in bacteria concentration created in *DV* flows occurs at higher level of the room. This is consistent with the literature [21] and can be explained by the stronger opposition to particle settling. The model was also able to predict reasonably the efficacy of the upper room *UVGI* since the relative error between the predicted and measured killing rates did not exceed 10%.

3.2. Experimental validation of the CFD model for bacteria deposition (for small droplets)

To evaluate the bacteria deposition in the room, the value from colony counting at each location was normalized by dividing it by the set experimental average. It was assumed that each *CFU* arises from a single viable microorganism.

The normalized bacteria count at a certain location i can be described by the following formula:

$$\overline{c_i} = \frac{c_i}{\frac{1}{n}\sum_{j=1}^{n} c_j} \tag{16}$$

where n is the total number of petri dishes.

A comparable normalization approach was adopted in analyzing simulation results to enable direct comparison between *CFD* and experimental spatial deposition patterns. Normalized experimental deposition values are presented together with *CFD* predictions at the twelve sampling plates are shown in Fig. 6. The *CFD* predictions of the number of droplet nuclei deposited on the petri plates are in good agreement with the *CFU* counts obtained experimentally with a relative error less than 15% at most of the sampling points. The minimal relative error at the mentioned points was 7% for the low supply flow rate and 2% for the high flow rate. The counting of the bacteria from the agar plates was done by experts in the microbiological lab. The CFD simulations used 100,000 trajectories to ensure accurate concentration predictions of the model. Similar accuracy in CFD results were reported by King et al. [38].

The distribution map of *S. marcescens* on the sampling plane (V) predicted by the *CFD* simulations of Experiments I and II are shown in Fig. 7. The plots show that the use of two 18 W UVC lamps reduced remarkably the bacteria concentration in the room. The transmission of bacteria from the source to distant occupants was reduced as well.

3.3. CFD substantiation of the simplified model (for large droplets)

The experimentally validated *CFD* model is reliable in predicting the deposition of pathogen-carrying particles of different sizes. It can then be used to substantiate the mathematical model for the case of large particles. For this reason, experimental scenarios 1 and 2 were simulated using the *CFD* and mathematical model using a particle size of 20 μm (equilibrium diameter) and maintaining the other simulation parameters unchanged. The simulation run of the MATLAB code of the simplified model takes about 5 min using a 4-core computer; whereas the computational time for a simulation

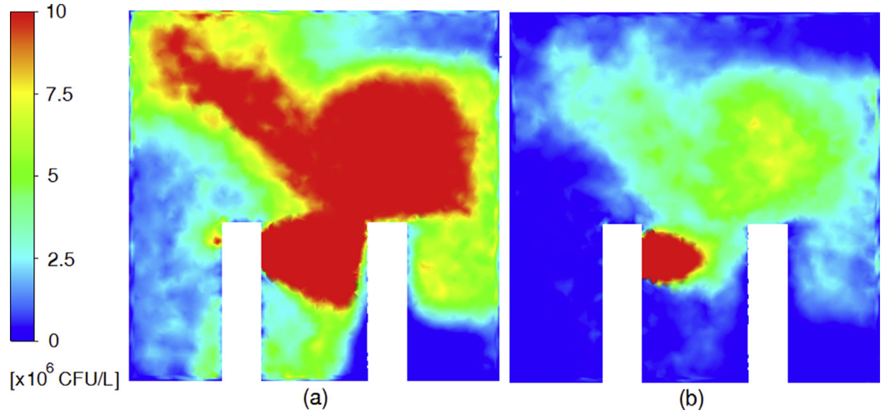

Fig. 7. *S. marcescens* concentration contour plots on the sampling plane for $m_s = 0.11$ kg/s (a) when UVGI is off and (b) when *UVGI* is on.

run of the *CFD* model in the Lagrangian domain is about 18 h on the same computer.

The predictions of airborne bacteria from the two models were then compared and shown in Fig. 8 where good agreement with maximal relative error of 10% was obtained. It can be concluded that the mathematical model is able to predict reasonably the transport of pathogens carried by large droplets as well. The comparison of the results obtained from the model not including the deposition effects with the *CFD* results for large droplets of 20 μm showed relative error up to 19%.

3.4. Effect of the droplet size

In order to study the effect of the droplet size on the pathogen transport in *UVGI* spaces conditioned by *CC/DV* system, the validated model was applied on the same experimental room for 4 different droplet equilibrium diameters: 2.5 μm, 10 μm, 15 μm, and 20 μm. The simulations runs were performed with and without the use of *UVGI* for *DV* flow rate of 0.11 kg/s and bacteria emission rate of 1400 CFU/min from an infected person by talking and coughing.

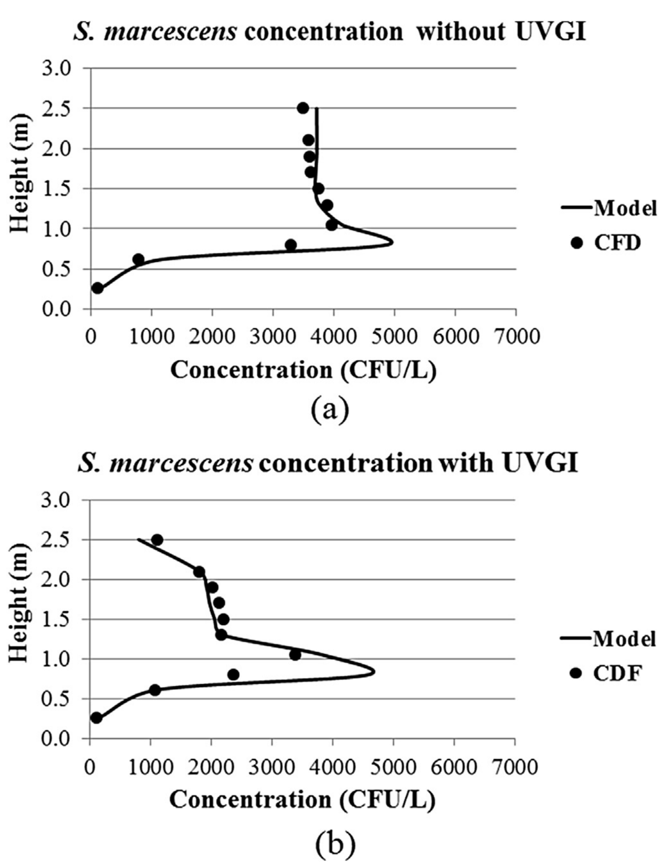

Fig. 8. Plots of bacteria concentration using the multi-layer model and the CFD simulation predictions as a function of height for room air (a) without the use of *UVGI* and (b) with the use of *UVGI*.

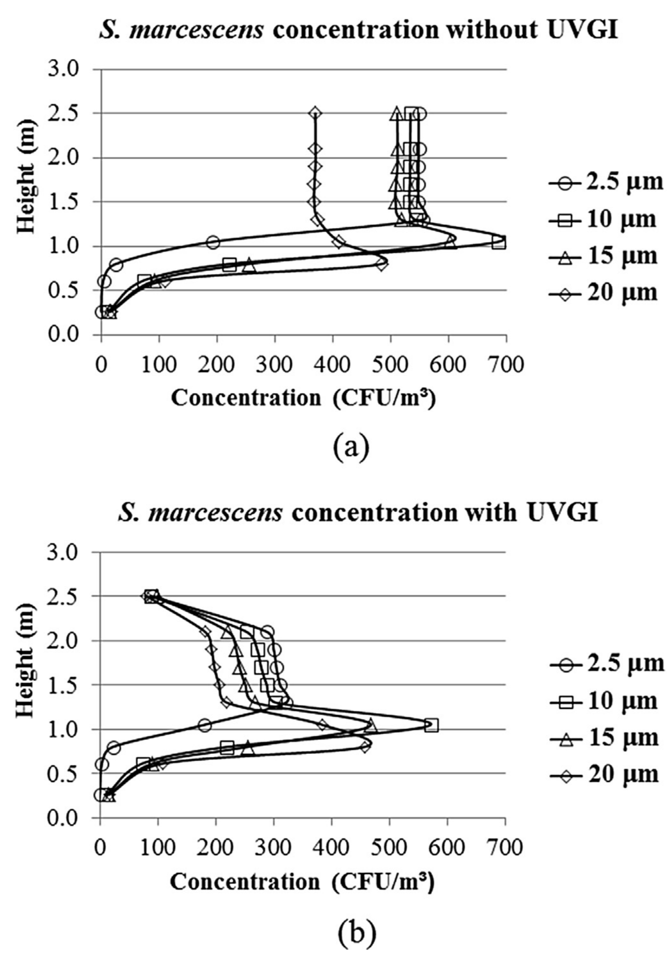

Fig. 9. Variations of bacteria concentration with height for droplet sizes 2.5, 10, 15, and 20 μm with and without the use of *UVGI*.

The variations of bacteria concentration with height and droplet equilibrium size are shown in Fig. 9. As the droplet diameter increases, the effect of gravitational settling increases and results in a drop in the exhaust concentration. Moreover, the maximal bacteria concentration increases with the droplet diameter for droplet size up to 10 μm. For larger droplets, settling onto floor and other horizontal surfaces occurs quickly, and the maximal bacteria concentration begins to decrease when the droplet size exceed 10 μm. Floor deposition played a significant role in reducing bacteria exposure only for droplets larger than 10 μm. The deposition of droplets on the floor acts against the principle of *DV* system featured with the reduction of contaminants in the occupied zone by entraining them into the upward buoyant flows. Deposition on the floor would not then play a positive role in particle removal unless it overcomes the upward flow in the surrounding air established by the *DV* system below the stratification height.

As seen also in Fig. 9, the maximal concentration occurs at the stratification height for droplet size 2.5 μm and below this level for larger droplets as was also found by Habchi et al. [21]. This finding can be explained by the increase in the gravitational settling that opposes the upward flow below the stratification level. In this case, unhealthy air quality is likely to occur in the occupied zone and the return air mixing ratio should be at its minimum. The use of upper room *UVGI* is then highly recommended to allow higher fractions of return air and then achieve more energy savings on the system. Results also show that the disinfection rate in the upper zone decreases from 88% to 78% as the size of pathogen-carrying particles increases from 2.5 μm to 20 μm. This can be explained by the fact that more bacteria were removed by deposition of large carrying particles, which reduces the percentage of bacteria removed by *UV* irradiation.

4. Conclusion

The transport of airborne bacteria in *CC/DV* rooms equipped with upper room *UVGI* systems was studied by experimentation, *CFD* and mathematical modeling. In the experimental study, the bacterial concentration was measured using steady-state air sampling method, and deposition was quantified using petri plates. The measurements were used to validate the mathematical predictive model and *CFD* model using small particles for two different ventilation rates. Results showed good agreement between measurements and simulation results. The *CFD* model was then used to validate the mathematical model for the case of large pathogen-carrying particles. Many runs of the validated mathematical model were performed varying the droplet size to investigate the effect of this parameter on pathogen distribution in *CC/DV* spaces.

Results revealed that the maximal airborne bacteria concentration occurs at the stratification level in *CC/DV* rooms for droplet nuclei size, and below this level for larger droplets.

It can be also concluded that in presence of upper room *UVGI*, the mixed *CC/DV* system is capable of protecting occupants from both “airborne” and “droplet” disease transmission modes. The upward DV flow moves the pathogens to the upper irradiated zone where they recirculate and receive significant UV dose. The air in that zone is then effectively disinfected and can be recirculated in the room providing healthy air quality in the occupied zone. The performance of upper room *UVGI* is also affected by the droplet size since larger portion of bacteria will be removed by deposition in case of large pathogen carriers. The study shows that the *UVGI* disinfection rate in the upper zone dropped from 88% to 78% as the equilibrium diameter of the droplets increases from 2.5 μm to 20 μm. The validated simplified model can be used as a design tool that predicts, at low computational cost, the transport of airborne pathogens at different droplet sizes in mixed CC/DV systems coupled with upper room *UVGI*.

Acknowledgment

The authors would like to acknowledge the financial support of the Lebanese National Council for Scientific Research grant No. 21156-102549, the ASHRAE Senior Award No. 620040, and Mr. Mohamad Omar Mansour for conducting the experiments.

References

[1] Stetzenbach LD, Buttner MP, Cruz P. Detection and enumeration of airborne biocontaminants. Curr Opin Biotechnol 2004;15(3):170–4.
[2] Corbett EL, Watt CJ, Walker N, Maher D, Williams BG, Raviglione MC, et al. The growing burden of tuberculosis: global trends and interactions with the HIV epidemic. Arch Intern Med 2003;163(9):1009–21.
[3] World Health Organization. Indoor air quality: biological contaminants. Copenhagen, Denmark: World Health Organization; 1988. European Series n. 31.
[4] Bjørn E, Nielsen PV. Dispersal of exhaled air and personal exposure in displacement ventilated rooms. Indoor Air 2002;12:147–64.
[5] Price HVAC. Engineering Guide displacement ventilation. http://www.pricehvac.com/Catalog/SectionJ.
[6] Kanaan M, Ghaddar N, Ghali K, Araj G. New airborne pathogen transport model for upper-room UVGI spaces conditioned by chilled ceiling and mixed displacement ventilation: enhancing air quality and energy performance. Energy Convers Manag 2014;85:50–61.
[7] Noakes CJ, Beggs CB, Sleigh PA. Modeling the performance of upper room ultraviolet germicidal irradiation devices in ventilated rooms: comparison of analytical and CFD methods. Indoor Built Environ 2004;13:477–88.
[8] Sung M, Kato S. Method to evaluate UV dose of upper-room UVGI system using the concept of ventilation efficiency. Build Environ 2010;45:1626–31.
[9] Bolashikov ZD, Melikov AK. Methods for air cleaning and protection of occupants for airborne pathogens. Build Environ 2009;44:1378–85.
[10] Papineni RS, Rosenthal FS. The size distribution of droplets in the exhaled breath of healthy human subjects. J Aerosol Med 1997;10(2):105–16.
[11] Duguid JP. The size and duration of air-carriage of respiratory droplets and droplet-nuclei. J Hyg 1946;4:471–80.
[12] Loudon RG, Roberts RM. Relation between the airborne diameters of respiratory droplets and the diameter of the stains left after recovery. Nature 1967;213:95–6.
[13] Chao CYH, Wan MP, Morawska L, Johnson GR, Ristovski ZD, Hargreaves, et al. Characterization of expiration air jets and droplet size distributions immediately at the mouth opening. J Aerosol Sci 2009;40(2):122–33.
[14] Nicas M, Nazaroff W, Hubbard A. Toward understanding the risk of secondary airborne infection: emission of respirable pathogens. J Occup Environ Hyg 2005;2:143–54.
[15] Centers for Disease Control and Prevention. Guidelines for environmental infection control in health-care facilities. Atlanta, GA: Centers for Disease Control and Prevention; 2003.
[16] Morawska L. Droplet fate in indoor environments, or can we prevent the spread of infection? Indoor Air 2006;16(5):335–47.
[17] Wan MP, Chao CYH, Ng YD, Sze To GN, Yu WC. Dispersion of expiratory droplets in a general hospital ward with ceiling mixing type mechanical ventilation system. Aerosol Sci Technol 2007;41(3):244–58.
[18] Wells WF. On air-borne infection. Study II. Droplets and droplet nuclei. Am J Hyg 1934;20:611–8.
[19] Hathway EA, Noakes CJ, Sleigh PA, Fletcher LA. CFD simulation of airborne pathogen transport due to human activities. Build Environ 2011;46:2500–11.
[20] Heidarinejad M, Srebric J. Computational fluid dynamics modeling of UR-UVGI lamp effectiveness to promote disinfection of airborne microorganisms. World Rev Sci Technol Sustain Dev 2013;10(1/2/3):78–95.
[21] Habchi C, Ghali K, Ghaddar N. A simplified mathematical model for predicting cross contamination in displacement ventilation air-conditioned spaces. J Aerosol Sci 2014;76:72–86.
[22] Gold E, Nankervis GA. Cytomegalovirus. In: Evans A, editor. Viral infections of humans. New York: Plenum Medical Book Co; 1989. p. 997–1002.
[23] McCluskey R, Sandin R, Greene J. Detection of airborne cytomegalo virus in hospital rooms of immune-compromised patients. J Virol Methods 1996;56:115–8.
[24] Ayoub M, Ghaddar N, Ghali K. Simplified thermal model of spaces cooled with combined chilled ceiling and displacement ventilation system. HVAC R Res 2006;12:1005–30.
[25] Goodfellow HD. Industrial ventilation design guidebook. San Diego, California, USA: A Harcourt Science and Technology Company; 2001.
[26] Mundt E. The performance of displacement ventilation system. Sweden: Royal Institute of Technology; 1996 (Ph.D. thesis).
[27] Jaluria Y. Natural convection. Pergamon Press Oxford; 1980.
[28] Lai ACK, Nazaroff WW. Modeling indoor particle deposition from turbulent flow onto smooth surfaces. J Aerosol Sci 2000;31(4):463–76.

[29] Chen Q, Xu W. A zero-equation turbulence model for indoor airflow simulation. Energy Build 1998;28(2):137–44.
[30] Wu CL, Yang Y, Wong SL, Lai ACK. A new mathematical model for irradiance field prediction of upper-room ultraviolet germicidal systems. J Hazard Mater 2011;189:173–85.
[31] Rahn RO, Xu P, Miller SL. Dosimetry of room-air germicidal (254 nm) radiation using spherical actinometry. Photochem Photobiol 1999;70(3):314–8.
[32] Ko G, First M, Burge H. Influence of relative humidity on particle size and UV sensitivity of *Serratia marcescens* and *Mycobacterium bovis BCG* aerosols. Tuber Lung Dis 2000;80(4):217–28.
[33] Keblawi A, Ghaddar N, Ghali K, Jensen L. Chilled ceiling displacement ventilation design charts correlations to employ in optimized system operation for feasible load ranges. Energy Build 2009;41(11):1155–64.
[34] Miller SL, Macher JM. Evaluation of a methodology for quantifying the effect of room air ultraviolet germicidal irradiation on airborne bacteria. Aerosol Sci Technol 2000;33(3):274–95.
[35] Wang B, Zhang A, Sun JL, Liu H, Hu J, Xu LX. Study of SARS transmission via liquid droplets in air. J Bio Mech Eng 2005;127:32–8.
[36] Goldman E, Green LH. Practical handbook of microbiology. 2nd ed. USA: CRC Press, Taylor and Francis Group; 2008. ISBN 978-0-8493-9365-5.
[37] Ariff M, Salim MS, Cheah SC. Wall y^+ approach for dealing with turbulent flow over surface mounted cube: part2-high Reynolds number. In: Seventh international conference on CFD in the minerals and process industries CSIRO, Melbourne, Australia; December 9-11, 2009.
[38] King MF, Noakes CJ, Sleigh PA, Camargo-Valero MA. Bioaerosol deposition in single and two-bed hospital rooms: a numerical and experimental study. Build Environ 2013;59:436–47.